



## Galvanostatic anodization of pure Al in some aqueous acid solutions Part I: Growth kinetics, composition and morphological structure of porous and barrier-type anodic alumina films

S.S. ABDEL REHIM, H.H. HASSAN and M.A. AMIN\*

Chemistry Department, Faculty of Science, Ain Shams University, Cairo, Egypt

(\*author for correspondence, e-mail: maaismail@yahoo.com)

Received 24 October 2001; accepted in revised form 24 July 2002

**Key words:** aluminium, anodizing acid solution, combined barrier/porous oxide growth

### Abstract

The growth kinetics of anodic films formed on the surface of high purity Al by anodization under galvanostatic conditions at current densities in the range 5–75 mA cm<sup>-2</sup> in thermostatically controlled and vigorously stirred solutions of chromic, sulfuric, phosphoric, citric, tartaric and oxalic acids at different temperatures, were studied. It has been shown that chromic acid solution produces a typical barrier type oxide growth at any given temperature, while the specific kinetic curve representing the combined barrier/porous type film growth is observed when the anodization process is carried out in a nonstirred chromic acid solution. The oxide growth in the rest of the anodizing solutions occurs in different ways depending on the bath temperature. Barrier oxide growth is observed at temperatures lower than 30 °C. Above this temperature, combined barrier/porous oxide growth is observed. In all cases, the slope of the linear part of the potential against time curves, and therefore the rate of barrier oxide growth, increases with increasing anodizing current density and acid concentration, while it decreases with increase in temperature. The composition and surface morphology of the anodic films have been studied by X-ray photoelectron spectroscopy (XPS), scanning electron microscopy (SEM), and atomic force microscopy (AFM).

### 1. Introduction

One of the attractive features of anodic films on aluminium is the flexibility of their properties. By choice of anodizing condition, especially electrolyte composition, oxide films with structure, hardness, chemical composition etc. varying over a wide range can be obtained [1]. The most popular electrolytes for anodization are aqueous solutions of chromic, sulfuric, oxalic, citric and tartaric acids. Among these chromic acid is of interest due to the peculiarities of the anodization process and the properties of the oxides obtained [2].

Anodic alumina films grown in aqueous electrolytes have either barrier or porous structures. A barrier oxide is a layer of uniform thickness that supports a high electric field [3]. The structure of porous anodic Al<sub>2</sub>O<sub>3</sub> film has been described as a close-packed array of columnar hexagonal cells each of which contains an elongated pore normal to the metal substrate surface and separated from it by a thin barrier type film layer [4, 5].

Parkhutik et al. [6, 7] investigated the growth kinetics and the morphology and structure of anodic films formed by anodic oxidation of Al in chromic acid and/or sulfuric acid under galvanostatic conditions, using

high-resolution transmission electron microscopy, ultra-soft X-ray spectroscopy and thermal derivatography. The authors reported that, at low current densities, porous oxide is formed, while higher current densities promote barrier type oxide formation. The anodic oxides formed in these solutions are amorphous and contain a mixture of AlO<sub>4</sub> tetrahedral and AlO<sub>6</sub> octahedral.

Patermarakis et al. [4] and others [3, 8–10] studied the growth kinetics of porous anodic films on Al metal under galvanostatic conditions in two acid solutions, namely 15% w/v H<sub>2</sub>SO<sub>4</sub> and H<sub>3</sub>PO<sub>4</sub> under stirring conditions at bath temperatures in the range 20–40 °C. The authors used SEM, Faraday's law, and oxide film mass measurements to analyse the growth kinetics and obtain film growth rates, pore density and porosity. The authors found that the rate of growth of porous anodic Al<sub>2</sub>O<sub>3</sub> films increases with increasing anodization time, current density and bath temperature.

This paper reports an investigation of the kinetics of thickness growth, morphology and structure of anodic films formed by anodic oxidation of Al under galvanostatic conditions in thermostatically controlled and vigorously stirred solutions of chromic, sulfuric, phosphoric, citric, tartaric and oxalic acids, for a range of anodizing conditions.

## 2. Experimental details

Aluminium oxide films were prepared by anodizing specimens of Al cut from a sheet (provided from the Egyptian Aluminium Company) 0.50 mm thick of the following chemical composition (wt %): Al 99.79%, Cu 0.05%, Mg 0.05%, Si 0.05%, Mn 0.05% and Zn 0.01%. The specimens were washed with distilled water, rinsed with ethanol, degreased with acetone, and then polished chemically using warmed chromophosphoric acid solution (20 g pure chromic acid powder and 35 cm<sup>3</sup> phosphoric acid (85.6 wt %) mixed with distilled water to make 1 L) followed by electrochemical polishing using a 1:1 by volume solution of (85.6 wt %) phosphoric acid and glacial acetic acid.

The anodizing process was carried out under galvanostatic conditions in aerated thermostatically controlled and vigorously stirred solutions of chromic, sulfuric, phosphoric, oxalic, citric and tartaric acids, at different values of the anodizing parameters, that can affect the properties and characteristics of the oxide film, such as acid concentration, bath temperature and current density. In these experiments the variation of potential with the anodization time was recorded using a potentiostat (potentiostat/galvanostat EG&G model 273) connected with a personal computer.

In the present work, the anodizing solution was well stirred to obtain an essentially uniform film thickness. In addition, vigorous stirring assures that the bath temperature and the anodizing temperature (temperature around pore bases during anodization) are, to a good approximation, the same [11, 12]. After anodization, each sample was washed thoroughly with distilled water and dried in a desiccator. The composition and surface morphology of the anodic oxide films were determined by employing X-ray photoelectron spectroscopy (XPS), scanning electron microscopy (SEM) and atomic force microscopy (AFM), respectively. The XPS spectrometer was a VG Escalab MKII with a MgK<sub>α</sub> X-ray source of 1235.6 eV with resolution of 0.20 eV at a constant analyser pass energy of 20 eV. AFM studies were performed with a multimode microscope stand controlled by Nanoscope III electronics, both from Digital Instruments. The tapping mode AFM probes were made of silicon and microfabricated by nanosensors. The SEM studies were carried out using Jeol-Jem-1200 EX II electron microscope.

## 3. Results and discussion

### 3.1. Kinetics of the oxide growth

To study the growth kinetics of the anodic films formed on the surface of pure Al, Al specimens were anodized galvanostatically at current densities (5–75 mA cm<sup>-2</sup>) in thermostatically controlled and vigorously stirred 1.0 M solutions of chromic, sulfuric, phosphoric, citric, tartaric and oxalic acid at different temperatures. Figure 1 (as

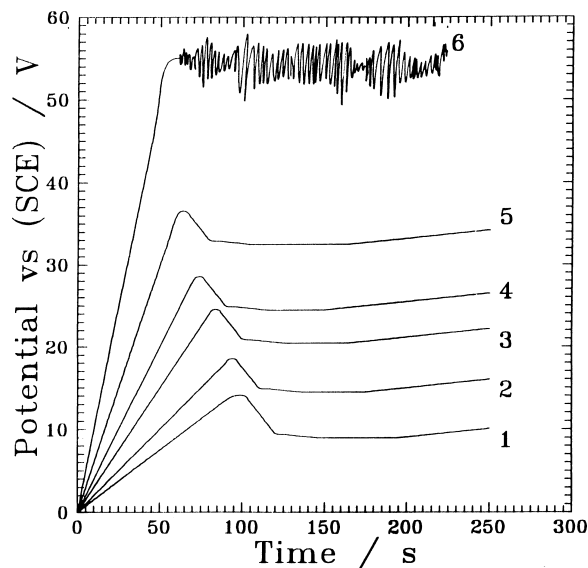


Fig. 1. Dependence of anodic potential on time for the anodization of aluminium in 1.0 M chromic, sulfuric, phosphoric, citric, tartaric and oxalic acid solutions at 30 °C and 25 mA cm<sup>-2</sup>. Key: (1) oxalic, (2) tartaric, (3) citric, (4) phosphoric, (5) sulfuric and (6) chromic acid.

an example) shows the dependence of the anodic potential on time for Al anodization in 1.0 M solutions at bath temperature of 30 °C and at a current density of 25 mA cm<sup>-2</sup>.

It is seen that anodization of Al in chromic acid solution produces a typical barrier oxide growth, since the kinetics reveal a linear rise in potential, and therefore an increase in its thickness with time up to the moment of dramatic potential oscillation (to the moment of electrical breakdown) [13]. Barrier type anodic alumina films develop by migration of O<sup>2-</sup> ions inwards across the preexisting oxide film under a relatively high electric field and their reaction with the Al at the metal/oxide interface [14–17]. The probable mechanism of ionic movement is a place exchange of oxygen and aluminium ions [18].

On the other hand, the potential against time transients obtained for the rest of the anodizing acid solutions show an initial linear increase, and then the potential reaches a maximum value before declining to a reasonably steady value. In the steady state region, the anodic film thickens relatively uniformly with time and the major anodic film parameters are directly proportional to the voltage [14]. These observations are consistent with the classical trend of potential against time that has been reported by others [19]. This trend is characteristic of combined barrier/porous oxide growth. It follows from the data of Figure 1 that the rate of potential increase, the value and location of potential maximum and the potential values following the decline from the maximum depend on the type of the anodizing solution. The slope of the linear part of the potential against time curves, and therefore the rate of barrier oxide growth for the six anodizing solutions decreases in the order: chromic > sulfuric > phosphoric >

citric > tartaric > oxalic acid. The sharp linear increase in potential at the commencement of anodization accompanies the initial formation of the barrier layer [19]. However, the higher the slope of the potential vs time, the higher the rate of barrier film formation. The decline in potential following the maximum corresponds to barrier layer thinning due to the nucleation and formation of pores [20]. After pore initiation, the porous film grows by continuous formation of the barrier layer as a result of the inward migration of  $O^{2-}$  anions and their reaction with the aluminium at the metal/oxide interface with cooperative migration of  $Al^{3+}$  ions outward under the field across the thickening film. The outwardly mobile  $Al^{3+}$  ions are ejected into the electrolyte from the pore base without forming solid alumina film [7]. In this case, a dynamic equilibrium is established between field assisted dissolution at the pore base and film growth at the metal/film interface. Therefore, an almost constant potential drop across the barrier layer, and constant thickness of the barrier layer during anodization are established. Cherki and Siejka [21] found that, for porous oxide growth in sulfuric acid, at least two-thirds of the Al in solution was the result of  $Al^{3+}$  ejected from the pore base. Therefore it follows from these data that the potential against time transient curves exhibit combined barrier/porous-type film growth kinetics.

The measured potential shown in the previous figures represents contributions from the potential drop in the bulk solution as well as the anodic potential, which is the potential drop across the porous and the barrier layer. The major contribution to the measured potential is the potential drop across the barrier layer, which explains the reasonably steady value observed following pore formation [8]. The slight increase in potential following pore formation can be attributed to the increasing film thickness.

### 3.1.1. Effect of anodizing current density

The influence of the anodizing current density on the growth kinetics of the anodic films on Al in all the thermostatically controlled and vigorously stirred 1.0 M solutions was studied at 30 °C. Results for chromic and sulfuric acid solutions are given in Figures 2 and 3, respectively.

Figures 2 and 3 show that the slope of the linear part of the potential against time curves increases with increasing current density up to less than about  $65 \text{ mA cm}^{-2}$ . This such behaviour is due to the increase in the rate of  $O^{2-}$  ion transport across the barrier layer toward the metal/oxide interface, where the formation of the barrier oxide takes place [13]. An increase in current density enhances the electric field across the barrier layer, and therefore increases the rate of ion transport. Thus, within this range of current densities, the higher the current density used, the higher the rate of barrier oxide growth. However, it is observed that higher current densities ( $\geq 65 \text{ mA cm}^{-2}$ ) are accompanied by a gradual increase in bath temperature. This

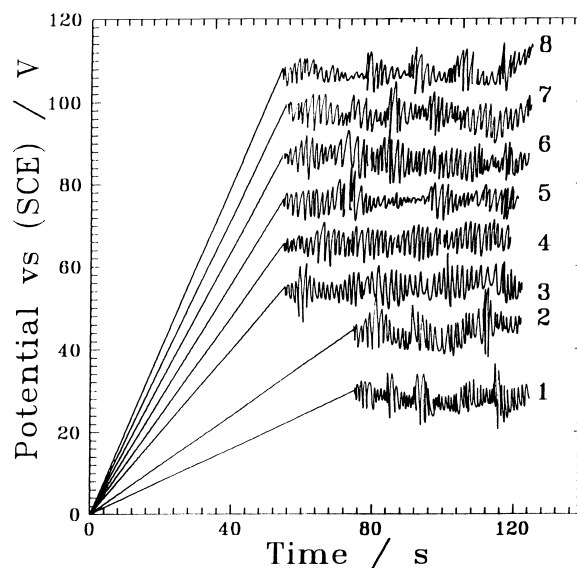


Fig. 2. Dependence of anodic potential on time for the anodization of aluminium in 1.0 M chromic acid solution at 30 °C and at different current densities: (1) 5, (2) 15, (3) 25, (4) 35, (5) 45, (6) 75, (7) 65 and (8)  $55 \text{ mA cm}^{-2}$ .

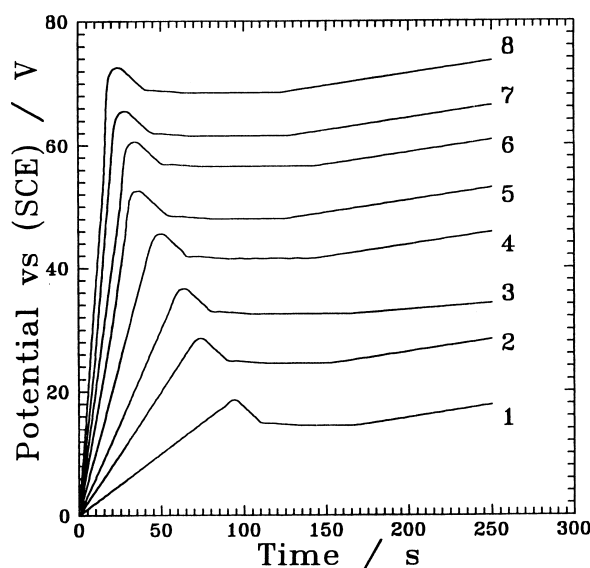


Fig. 3. Dependence of anodic potential on time for the anodization of aluminium in 1.0 M sulfuric acid solution at 30 °C and at different current densities: (1) 5, (2) 15, (3) 25, (4) 35, (5) 45, (6) 75, (7) 65 and (8)  $55 \text{ mA cm}^{-2}$ .

increase in temperature becomes the predominant factor and enhances the chemical dissolution of the barrier oxide layer. Therefore, the rise in temperature is responsible for the decrease in the initial slope of the linear part of the potential against time curves observed at current densities  $\geq 65 \text{ mA cm}^{-2}$  for all the cited acids. However, the use of such high current densities (for all the acids except for chromic acid) also results in an increase in the solution temperature inside the pores, even with vigorous stirring, and a sharp decrease in the recorded steady state potential is observed [20, 22]. (curves 6 and 7 in Figures 2 and 3).

### 3.1.2. Effect of acid concentration

Figures 4 and 5 present the effect of the concentration of the anodizing solution on the growth kinetics of anodic films on Al in chromic and sulfuric acid at  $25 \text{ mA cm}^{-2}$  and  $30^\circ\text{C}$ , respectively. The rest of the anodizing solutions gave results similar to those obtained for sulfuric acid presented in Figure 5.

Figures 4 and 5 demonstrate that the rate of potential increase, the value and location of the potential maximum, and the potential value following the decline from the maximum were dependent on electrolyte concentra-

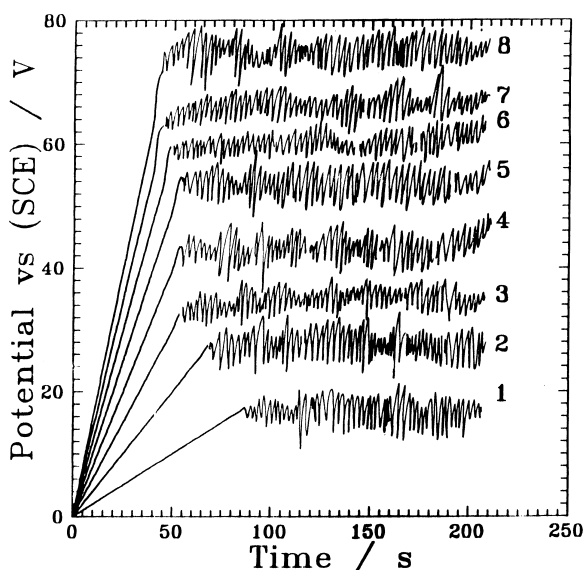


Fig. 4. Dependence of anodic potential on time for the anodization of aluminium in different concentrations of chromic acid solution at  $30^\circ\text{C}$  and  $25 \text{ mA cm}^{-2}$ . Concentration: (1) 0.05, (2) 0.10, (3) 0.25, (4) 0.50, (5) 1.00, (6) 6.00, (7) 4.00 and (8) 2.00 M.

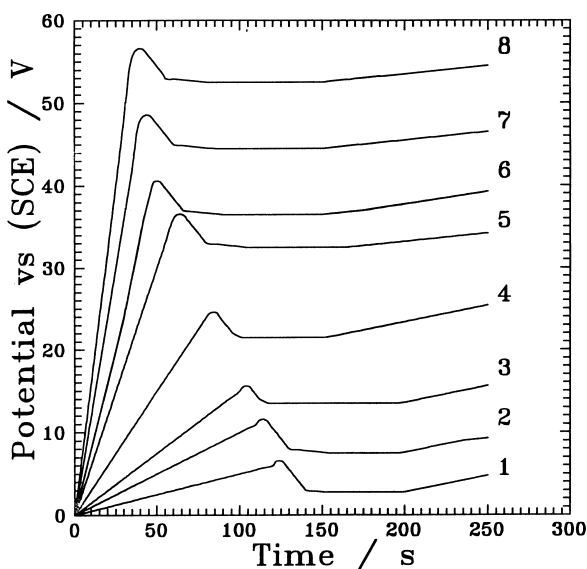


Fig. 5. Kinetic dependencies (anodic potential against time) for the anodization of aluminium in different concentrations of sulfuric acid solution at  $30^\circ\text{C}$  and at  $25 \text{ mA cm}^{-2}$ . Concentration: (1) 0.05, (2) 0.10, (3) 0.25, (4) 0.50, (5) 1.00, (6) 6.00, (7) 4.00, (8) 2.00 M.

tion. It is observed that in dilute solutions ( $<4.0 \text{ M}$ ), the slope of the linear part of the potential against time curves and, therefore, the rate of oxide growth, increase with increasing acid concentration. An increase in acid concentration results in an increase in solution conductivity. This increase in conductivity within this concentration range, may result in an increase in the rate of migration of  $\text{O}^{2-}$  ions across the barrier layer toward the metal/oxide interface, resulting in an increase in the oxide film thickness [13]. Nevertheless, the use of high concentrations ( $\geq 4.0 \text{ M}$ ) may be counterproductive, as shown by the curves 6 and 7 in both Figures 4 and 5, because the acid, while aiding oxide formation, promotes oxide dissolution [1], resulting in a decrease in film thickness.

### 3.1.3. Effect of temperature

In industry, the temperature of the anodizing acid solution plays an important role. For this reason, the influence of bath temperature on the growth kinetics of the anodic films on Al in 1.0 M solutions at a current density of  $25 \text{ mA cm}^{-2}$  was examined. The results show that anodization of Al in chromic acid solution at any temperature produces a typical barrier oxide. On the other hand, the growth kinetic curves for the rest of the anodizing solutions depend on the bath temperature, as shown in Figure 6 for sulfuric acid. In all cases, the slope of the linear part of the potential against time curves, and therefore the rate of the barrier oxide growth decreases with increasing temperature.

Figure 6 shows that the specific kinetic curve representing the combined barrier/porous oxide growth is observed at temperatures greater than  $30^\circ\text{C}$ . At lower temperatures, barrier oxide is presumably formed, similar to that observed in chromic acid, whereas higher temperatures favour porous structure formation. The

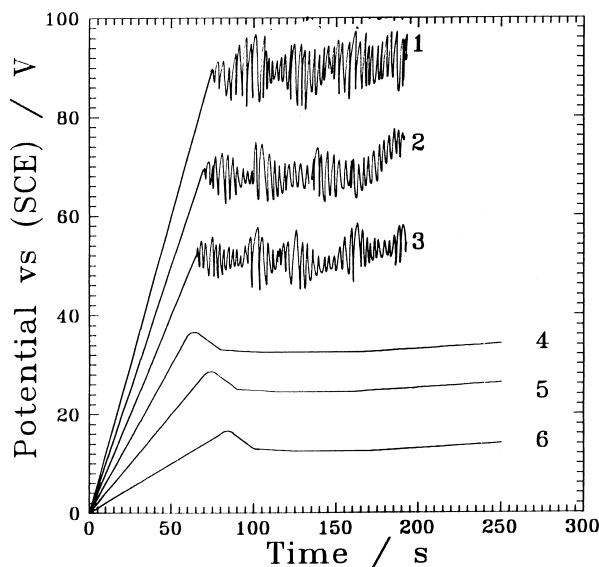


Fig. 6. Dependence of anodic potential on time for the anodization of aluminium in 1.0 M sulfuric acid solution at  $25 \text{ mA cm}^{-2}$  and different temperatures: (1)  $5^\circ\text{C}$ , (2)  $10^\circ\text{C}$ , (3)  $20^\circ\text{C}$ , (4)  $30^\circ\text{C}$ , (5)  $50^\circ\text{C}$ , (6)  $60^\circ\text{C}$ .

influence of temperature on the transition from barrier to combined barrier/porous oxide growth may be explained on the basis of the fact that the low temperature does not promote oxide dissolution and so the transition from barrier to combined barrier/porous oxide growth is retarded. Increase in electrolyte temperature, on the other hand, enhances oxide dissolution [1], and therefore promotes transition from barrier to combined barrier/porous oxide growth. Increase in temperature also enhances chemical dissolution along the pore base, as well as the pore walls, resulting in an increase in the pore volume.

### 3.1.4. Effect of stirring

The effect of stirring on growth kinetics on Al in 1.0 M anodizing acid solutions at  $25 \text{ mA cm}^{-2}$  and  $30^\circ\text{C}$  was studied. The results demonstrated that bath stirring has a pronounced effect on the growth kinetics. Figure 7 shows the results for chromic acid solution. When the solution is stirred, a typical barrier oxide growth is observed (curve 1), while the specific kinetic curve representing the combined barrier/porous growth is observed when anodization is carried out in a nonstirred chromic acid solution.

Inspection of the data of Figure 7, as well as that obtained for the rest of the anodizing acid solutions, reveals that the slopes of the linear parts of the potential time curves, and therefore the rates of oxide film growth, are higher in stirred solution than in non-stirred. These results may be explained on the basis that anodizing is an extremely exothermic reaction, accompanied by heat release. The evolved heat is due to both the energy of reaction between Al and oxygen and the Joule phenomenon. High temperatures and absence of bath stirring causes the following changes: (i) oxide has too large pores which are difficult to seal, and (ii) the dissolving

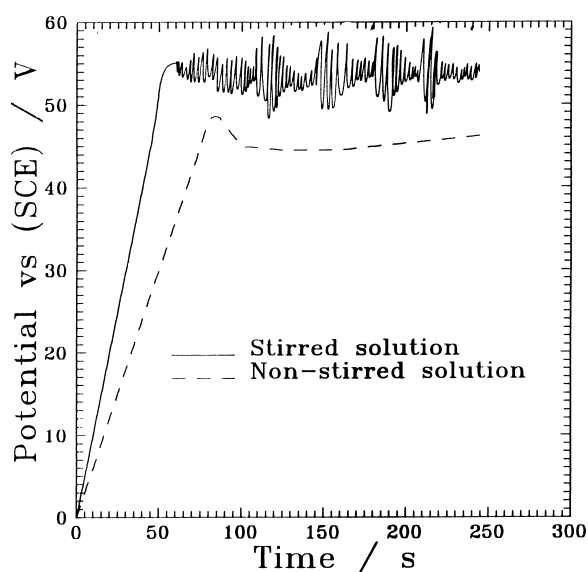


Fig. 7. Influence of bath stirring on anodic potential against time plot for the anodization of aluminium in 0.50 M chromic acid solution at  $25 \text{ mA cm}^{-2}$  and at a temperature of  $30^\circ\text{C}$ .

ability of the acid on the oxide increases, thus promoting the transition from barrier to combined barrier/porous oxide growth.

### 3.1.5. Effect of adding oxalic acid to sulfuric acid solution

In industry, additives are added to sulfuric acid solution to improve the anodization process. The most common one is oxalic acid, which has the advantages of reducing oxide dissolution and producing less porous, harder and more compact oxide.

The effect of adding increasing amounts of oxalic acid to 0.50 M of the employed anodizing acid on the growth kinetics of anodic films on Al at a given current density and temperature was examined; Figure 8 is a representative example in 0.50 M sulfuric acid solution. The slope of the linear part of the potential against time curves, and therefore the rate of barrier oxide film growth, increases with increasing oxalic acid concentration. In addition, the rate of potential rise, the value and location of the potential maximum, and the potential following the decline from the maximum were found to be dependent on oxalic acid concentration. Therefore, it can be concluded that the presence of oxalic acid reduces oxide dissolution and produces less porous and more compact oxide film.

### 3.2. Chemical composition and surface morphology of the oxide layer

The chemical composition and morphological structure of the films formed on Al in thermostatically controlled and vigorously stirred solutions of chromic, sulfuric, phosphoric, citric, tartaric and oxalic acids at  $25 \text{ mA cm}^{-2}$  and  $30^\circ\text{C}$  was studied by X-ray photoelectron

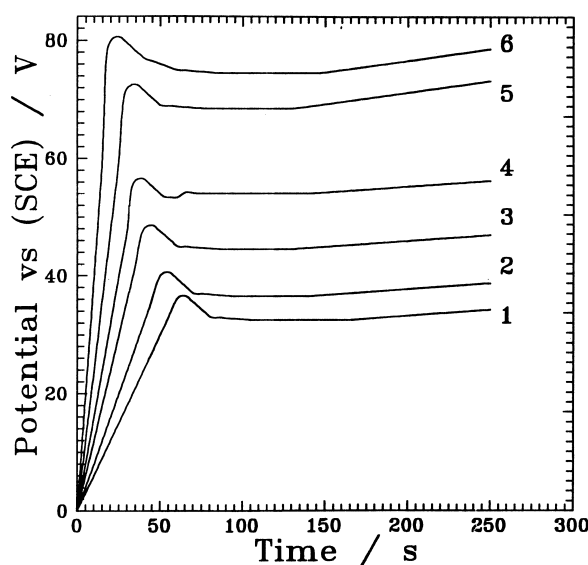


Fig. 8. Dependence of anodic potential on time for the anodization of aluminium in 0.50 M sulfuric acid solution in the absence and presence of oxalic acid at different concentrations at  $25 \text{ mA cm}^{-2}$  and at  $30^\circ\text{C}$ . Concentration: (1) 0.000, (2) 0.005, (3) 0.010, (4) 0.050, (5) 0.100 and (6) 0.200 M.

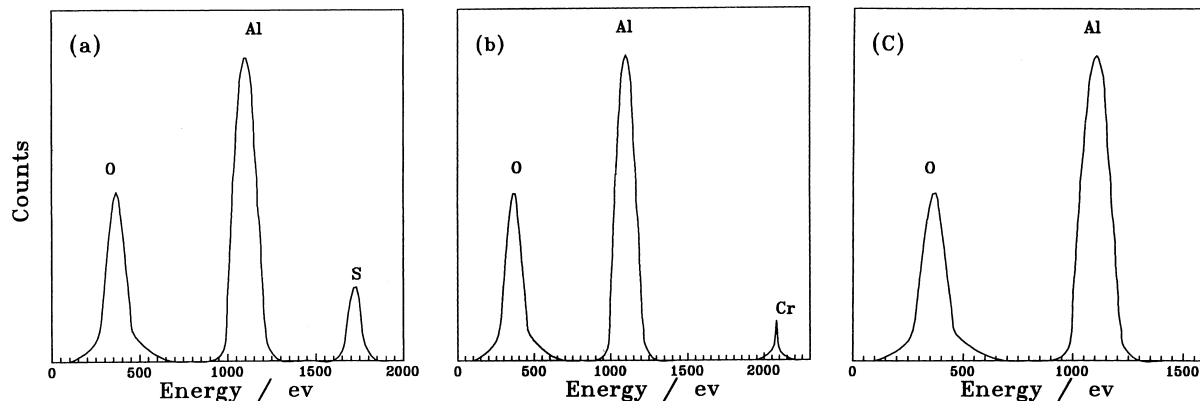


Fig. 9. XPS spectral lines of an anodic alumina layer galvanostatically grown on the surface of aluminium as anodized in 1.0 M (a) sulfuric, (b) chromic and (c) phosphoric acid solutions at  $25 \text{ mA cm}^{-2}$  and  $30 \text{ }^\circ\text{C}$ .

spectroscopy (XPS), scanning electron microscopy (SEM) and atomic force microscopy (AFM).

The oxide  $\text{Al}_2\text{O}_3$  formed in sulfuric acid contains a certain amount of sulfur (Figure 9(a)), presumably as sulfate ions, indicating a deep penetration of sulfate

anions into the oxide bulk and coincides with the results obtained by XPS [23], AES [24] and other methods [25]. The sulphate anions arise from incorporation of solution anions at the pore base/electrolyte interface during anodizing. At the same time, the  $\text{Al}_2\text{O}_3$  formed in

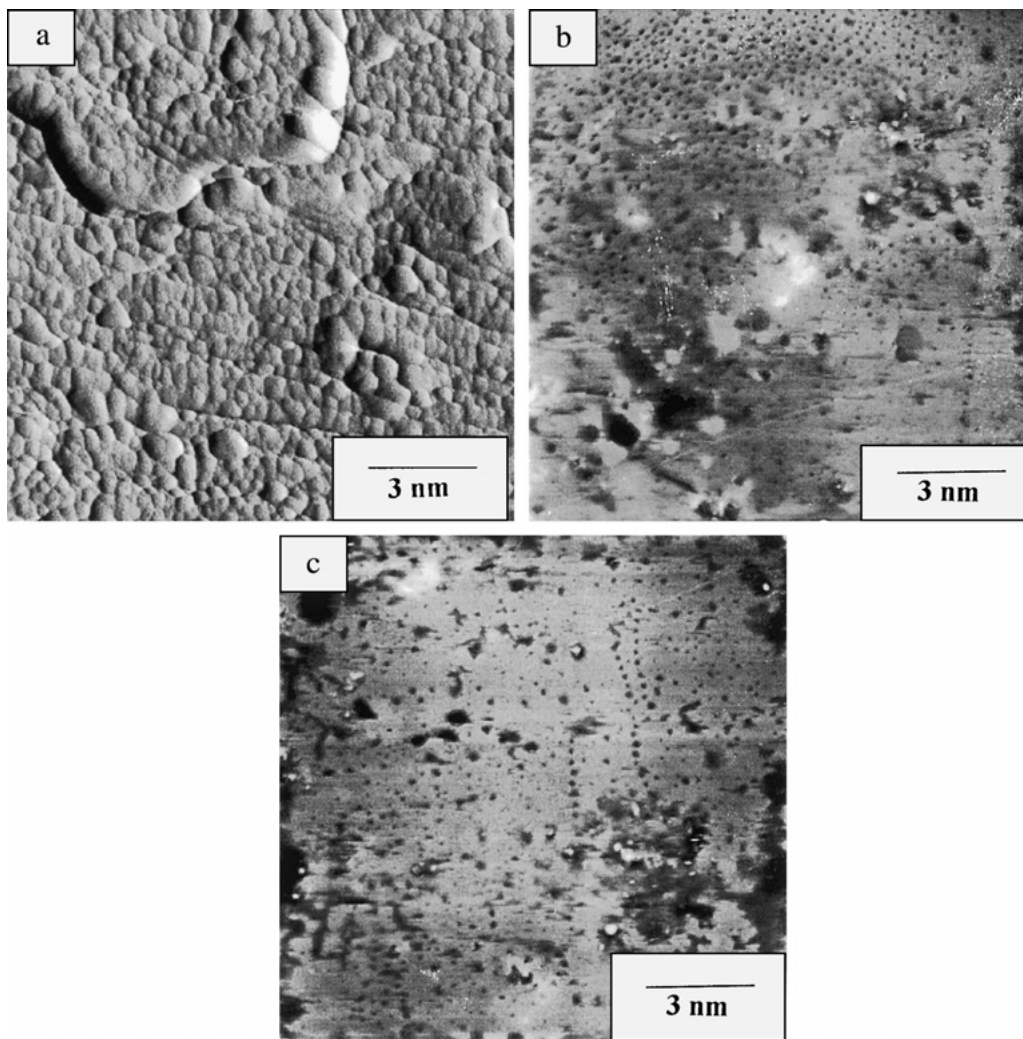


Fig. 10. SEM images of an anodic alumina layer galvanostatically grown on the surface of pure aluminium as anodized in 1.0 M (a) chromic, (b) sulfuric and (c) oxalic acid solutions at  $25 \text{ mA cm}^{-2}$  and  $30 \text{ }^\circ\text{C}$ .

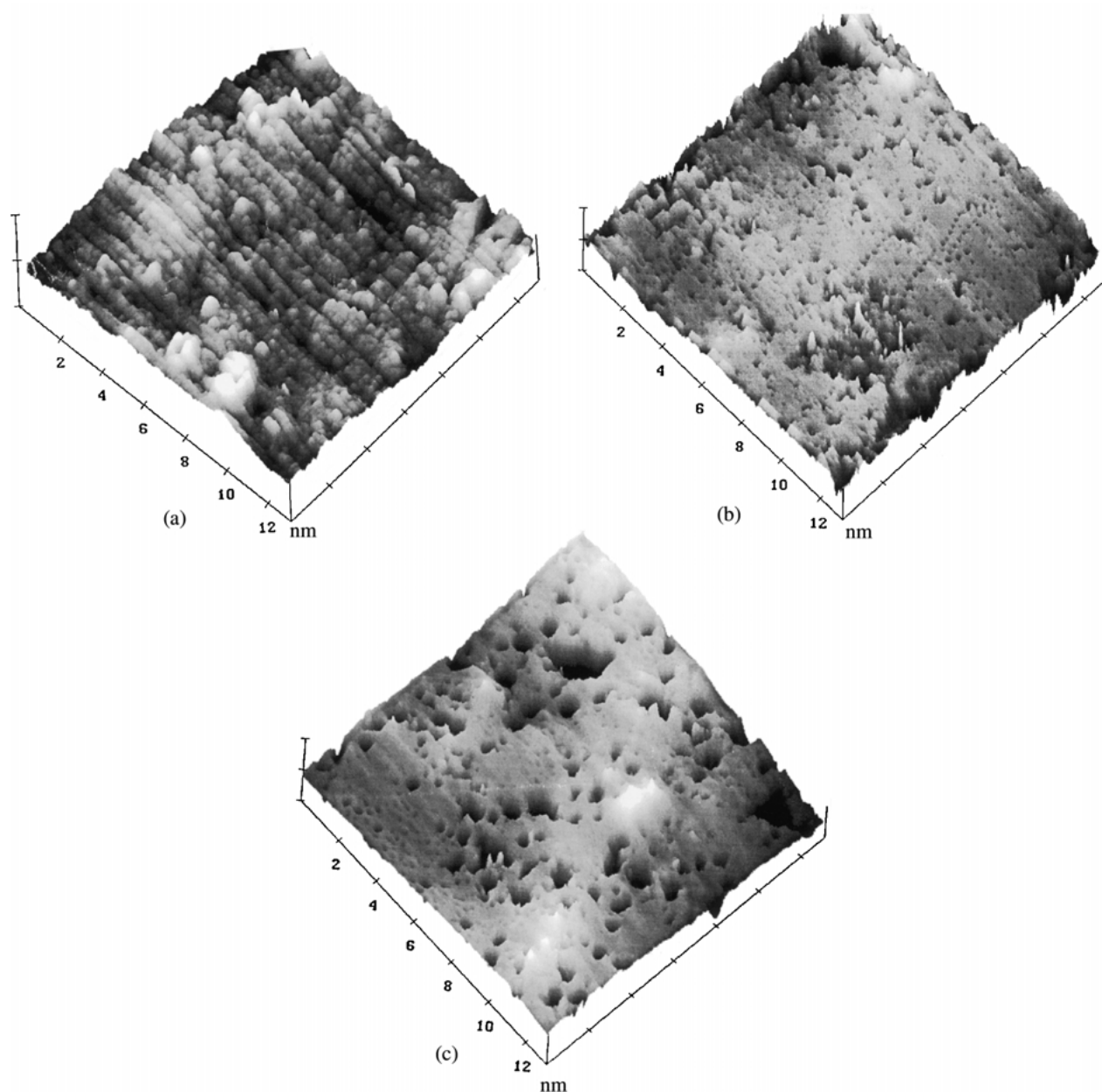


Fig. 11. ( $12 \times 12 \mu\text{m}$ ) AFM images (three-dimensional surface plots) of an anodic alumina layer galvanostatically grown on the surface of pure aluminium as anodized in 1.0 M (a) chromic, (b) sulfuric and (c) oxalic acid solutions at  $25 \text{ mA cm}^{-2}$  and  $30^\circ\text{C}$ .

chromic acid (Figure 9(b)) exhibits much less anion incorporation, confirming weak penetration of the chromate ions into the oxide bulk, indicating that the oxide layer in this case is of the barrier type [1, 2]. It is known that the chromate ions are more polarizable than sulfate ions, consequently, the chromate ions are adsorbed by the oxide surface more intensively than are the sulfate ions [6]. It is likely that the adsorption of chromate anions at the oxide surface inhibits its hydration through decreasing the number of adsorption sites available for water molecule adsorption and promotes the formation of surface phases like  $\text{Cr}_2\text{O}_3$ , which is more stable against dissolution in chromic acid [26]. This is a reason for retarding the porous oxide formation and enhancing the barrier type oxide forma-

tion in that solution as compared with sulfuric acid solution. On the other hand, Parkhutik et al. [7] suggested that adsorption of chromate ions on the oxide surface may inhibit the place exchange mechanism of Al movement outwards. In this case, new oxide layers should be formed at the metal oxide interface.

The SEM and AFM observations of the anodic alumina films (some examples are given in Figures 10 and 11, respectively) have confirmed that the structure of the oxide grown in chromic acid is nonporous as compared with that for oxides formed in the rest of the anodizing acid solutions. However, the data show clearly the presence of pores in the films grown in the rest of the acid solutions. It is seen that the pore density and width decrease in the order: oxalic > tartaric >

citric > phosphoric > sulfuric. The irregular surface morphology observed in the image of chromic acid solution is ensured, not by regular pore growth, but rather by electrolytic breakdown of the growing barrier oxide film.

#### 4. Conclusions

Chromic acid solution produces a typical barrier oxide growth at all temperatures. Sulfuric, phosphoric, tartaric, citric and oxalic acid solution produces a combined barrier/porous oxide growth. The slope of the linear part of the potential against time curves, and therefore the thickness of barrier oxide growth, increases with increasing current density up to less than about  $65 \text{ mA cm}^{-2}$  and concentration of the anodizing acid solution up to less than 4.0 M, while it decreases with increasing temperature.

The rate of barrier oxide growth for the anodizing acid solutions at the same anodizing conditions decreases in the order: chromic > sulfuric > phosphoric > citric > tartaric > oxalic acid. XPS data demonstrate that anodic alumina films formed in all the anodizing acid solutions have signals characteristic of Al and O. In the case of anodizing Al in chromic and sulfuric acid solutions additional XPS spectra lines were observed characteristic of Cr and S. In chromic acid, the adsorption of chromate anions at the oxide surface inhibit the formation of porous oxide film.

The SEM and AFM data confirm the suggestion that, in chromic acid only, a barrier type layer is produced, while in the other acid solutions combined barrier/porous type oxide films are obtained. The density and width of pores decreases in the order: oxalic > tartaric > citric > phosphoric > sulfuric.

#### References

1. A.R. Despic and V.P. Parkhutik, Electrochemistry of aluminium in aqueous solutions and physics of its anodic oxide, in J.O.'M. Bockris, B.E. Conway and R.M. White (Eds), 'Modern Aspects of Electrochemistry' Vol. 20 (Plenum Press, New York, 1989), p. 397.
2. S. Ono, S. Chiaki and T. Sato, *J. Met. Finish. Soc. Jpn.* **26** (1975) 26.
3. Y. Liu, R.S. Alwitt and K. Shimizu, *J. Electrochem. Soc.* **147** (2000) 1382.
4. G. Patermarakis and N. Papandreadis, *Electrochim. Acta* **38** (1993) 2351.
5. G. Patermarakis and K. Moussoutzanis, *J. Electrochem. Soc.* **142** (1995) 737.
6. V.P. Parkhutik, J.M. Albella, Yu.E. Makushok, I. Montero, J.M. Martinez-Duart and V.I. Shershulskii, *Electrochim. Acta* **35** (1990) 955.
7. V.P. Parkhutik, V.T. Belov and M.A. Chernyckh, *Electrochim. Acta* **35** (1990) 961.
8. A.T. Shawaqfeh and R.E. Baltus, *J. Electrochem. Soc.* **145** (1998) 2699.
9. K. Shimizu, R.S. Alwitt and Y. Liu, *J. Electrochem. Soc.* **147** (2000) 1388.
10. H. Uchi, T. Kanno and R.S. Alwitt, *J. Electrochem. Soc.* **148** (2001) B17.
11. Th. Skoulikidis and G. Patermarakis, *Aluminium* **65** (1989) 185.
12. G. Patermarakis and C. Pavlidou, *J. Catal.* **147** (1994) 140.
13. J.M. Albella, I. Montero and J.M. Martinez-Duart, *Electrochim. Acta* **32** (1987) 255.
14. M.A. Paez, T.M. Foong, C.T. NI, G.E. Thompson, K. Shimizu, H. Habazaki, P. Skeldon and G.C. Wood, *Corros. Sci.* **38** (1996) 59.
15. H. Habazaki, K. Shimizu, P. Skeldon, G.E. Thompson, X. Zhou, J. De Leat and G.C. Wood, *Corros. Sci.* **39** (1997) 719.
16. F. Brown and W.D. Mackintosh, *J. Electrochem. Soc.* **148** (2001) 1096.
17. G.E. Thompson, Y. Xu, P. Skeldon, K. Shimizu, S.H. Han and G.C. Wood, *Philos. Mag. B* **55** (1987) 651.
18. A.T. Fromhold and R.G. Fromhold, in C.H. Bamford (Ed.), 'Comprehensive Chemical Kinetics', Vol. 21 (Elsevier, Amsterdam, 1984), p. 1.
19. G.E. Thompson and G.C. Wood, in J.C. Scully (Ed.), 'Treatise on Materials Science and Technology', Vol. 23 (Academic Press, New York, 1983), p. 205.
20. G. Patermarakis and D. Tzouvelekis, *Electrochim. Acta* **39** (1991) 2419.
21. C. Cherki and J. Siejka, *J. Electrochem. Soc.* **120** (1973) 784.
22. J.P. O'Sullivan and G.C. Wood, *Proc. R. Soc. Lond. A.* **317** (1970) 511.
23. V.I. Nefedov, 'X-ray Photoelectron Spectroscopy of Chemical Compounds' (Khimiya, Moscow, 1984).
24. V.P. Parkhutik, *Corros. Sci.* **26** (1986) 295.
25. V.P. Parkhutik, Yu.E. Makushok and V.I. Shershulskii, in Proceedings of the International Symposium on 'Aluminium Surface Treatment Technology' (The Electrochem. Society, Pennington, NJ, 1986).
26. C. Edelen and U.R. Evans, *Trans. Faraday Soc.* **47** (1951) 1121.